J. Korean Math. Soc. **51** (2014), No. 6, pp. 1221–1250
http://dx.doi.org/10.4134/JKMS.2014.51.6.1221

KNOTS IN S^3 ADMITTING GRAPH MANIFOLD DEHN SURGERIES

Sungmo Kang

Abstract. In this paper, we construct infinite families of knots in S^3 which admit Dehn surgery producing a graph manifold which consists of two Seifert-fibered spaces over the disk with two exceptional fibers, glued together along their boundaries. In particular, we show that for any natural numbers a, b, c, and d with $a \geq 3$ and $b, c, d \geq 2$, there are knots in S^3 admitting a graph manifold Dehn surgery consisting of two Seifert-fibered spaces over the disk with two exceptional fibers of indexes a, b, and c, d, respectively.

1. Introduction

Let K be a knot in S^3, $N(K)$ a regular neighborhood of K in S^3, and $M_K = S^3 - \text{int}N(K)$. Let r be a slope, i.e., the isotopy class of an essential unoriented simple closed curve, on $\partial N(K)(= \partial M_K)$. There is a bijection between the set of slopes and $\mathbb{Q} \cup \{1/0\}$ in the usual way [11]. In particular, the slope of a meridian of K corresponds to $1/0$. The manifold obtained by r-Dehn filling is defined to be $K(r) = M_K \cup V$, where V is a solid torus glued to M_K along ∂M_K so that r bounds a meridian disk of V.

Let H be a genus two handlebody, k an essential simple closed curve in ∂H, and $H[k]$ the 3-manifold obtained by adding a 2-handle to H along k. We say k is *primitive* in H if $H[k]$ is a solid torus. Equivalently k is conjugate to a free generator of $\pi_1(H)$. Similarly, we say k is *Seifert* in H if $H[k]$ is a Seifert-fibered space and not a solid torus. Note that since H is a genus two handlebody, that k is Seifert in H implies that $H[k]$ is an orientable Seifert-fibered space over D^2 with two exceptional fibers, or an orientable Seifert-fibered space over the Möbius band with at most one exceptional fiber.

Suppose K is a knot in S^3 which lies in a genus two Heegaard surface Σ of S^3 bounding handlebodies H and H'. K in Σ is *primitive/primitive* or *double-primitive* if it is primitive with respect to both H and H'. Similarly, K is

Received March 10, 2014; Revised June 9, 2014.
2010 *Mathematics Subject Classification.* Primary 57M25.
Key words and phrases. knots, Dehn surgery, graph manifolds, Seifert curves, twisted torus knots, R-R diagrams.

primitive/Seifert if it is primitive with respect to one of H or H', and Seifert with respect to the other. Also K is *Seifert/Seifert* or *double-Seifert* if it is Seifert with respect to both H and H'.

In [1] using primitive curves Berge constructed 12 types of primitive/primitive knots and showed that these knots admit lens space surgeries. Dean generalized Berge's construction in his thesis [5], and its published version [6]. He introduced Seifert curves and described primitive/Seifert knots which have Dehn surgery producing a Seifert-fibered space over S^2 with three exceptional fibers.

Let γ be a component of $\partial N(K) \cap \Sigma$ which is an essential simple closed curve in $\partial N(K)$. Then the isotopy class of γ in $\partial N(K)$ defines the *surface slope* in $\partial N(K)$. (The surface slope depends on the embedding of K in Σ, so a knot in S^3 may have more than one surface slope.) Since the surface slope intersects a meridian of K in a single point, it is integral.

Lemma 1.1. *Let K be a knot lying in a genus two Heegaard surface Σ of S^3 bounding handlebodies H and H', and γ a surface slope with respect to this embedding of K. Then $K(\gamma) \cong H[K] \cup_\partial H'[K]$.*

Proof. It follows from Lemma 2.1 in [6]. □

Throughout this paper, we denote by $S(a_1, \dots, a_n)$ the Seifert-fibered space over a surface S with n exceptional fibers of indexes $a_1, \dots, a_n$.

Lemma 1.1 implies that primitive/primitive knots have a lens space surgery at a surface slope. While primitive/Seifert knots admit Dehn surgery producing $S^2(a, b, c)$, $\mathbb{R}\mathrm{P}^2(a, b)$, or a connected sum of lens spaces. However, due to Eudave-Muñoz [7] a connected sum of lens spaces cannot arise for hyperbolic primitive/Seifert knots. Hyperbolic primitive/primitive knots and primitive/Seifert knots are completely classified in [3].

Seifert/Seifert knots have Dehn surgery yielding $S^2(a, b, c, d)$, $\mathbb{R}\mathrm{P}^2(a, b, c)$, $K^2(a, b)$, or a graph manifold, where K^2 is a Klein bottle. However $K^2(a, b)$ cannot happen as Dehn surgery of knots in S^3 for homological reasons. In [9], using Seifert/Seifert knots the author gave infinite families of knots in S^3 which admit Dehn surgery producing $S^2(a, b, c, d)$. In this paper, we will focus on Seifert/Seifert knots admitting a graph manifold Dehn surgery which consists of $D^2(a, b)$ and $D^2(c, d)$, glued together along their boundaries. In [8] Eudave-Muñoz gave an infinite family of hyperbolic knots in S^3 admitting such a graph manifold Dehn surgery with slopes either half-integral or integral. Another infinite family of hyperbolic knots in S^3 was provided by Teragaito in [12], where each knot in the family admits three graph manifold Dehn surgeries corresponding to consecutive integers. However, both families of knots in [8] and [12] admit Dehn surgery producing a graph manifold consisting of $D^2(a, b)$ and $D^2(c, d)$ such that one of a, b, c and d is either 2 or 3. In this paper, we show the following.

Theorem 1.2. *There are infinite families of Seifert/Seifert knots in S^3 admitting a graph manifold Dehn surgery consisting of $D^2(a,b)$ and $D^2(c,d)$. Furthermore, for any natural numbers $a, b, c,$ and d with $a \geq 3$ and $b, c, d \geq 2$, there are Seifert/Seifert knots in S^3 admitting a graph manifold Dehn surgery consisting of $D^2(a,b)$ and $D^2(c,d)$.*

2. Twisted torus knots which are Seifert/Seifert curves

In this section, using twisted torus knots we construct Seifert/Seifert knots. Since twisted torus knots are originally introduced by Dean in [6], we go through the definitions and statements in [6].

Let $G_{a,b} = \langle x, y \mid x^a y^b \rangle$ be a group presentation with two generators x, y and one relator $x^a y^b$. An element w in the free group $\langle x, y \rangle$ is said to be (a,b) *Seifert-fibered* if $\langle x, y \mid w \rangle$ is isomorphic to $G_{a,b}$.

Lemma 2.1. *Let k be a simple closed curve in the boundary of a genus two handlebody H. k is a Seifert curve in H with $H[k] = D^2(a,b)$ if and only if k in $\pi_1(H)$ is (a,b) Seifert-fibered.*

Proof. This is Lemma 2.2 in [6]. □

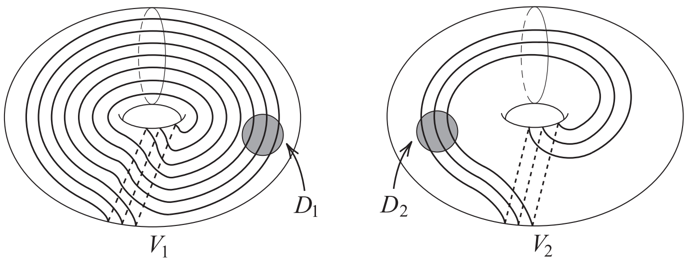

FIGURE 1. The $(7,3)$-torus knot $T(7,3)$ and 3 parallel copies $3T(1,1)$ of the $(1,1)$-torus knot.

Now we construct twisted torus knots as follows. Let V_1 and V_2 be standardly embedded disjoint unlinked solid tori in S^3. Let $T(p,q)$ be the (p,q)-torus knot which lies in the boundary of V_1. Let $rT(m,n)$ be the r parallel copies of the (m,n)-torus knot $T(m,n)$ which lies in the boundary of V_2. Here we may assume that $1 \leq q < p$ and $m > 0$. Let D_1 be the disk in ∂V_1 so that $T(p,q)$ intersects D_1 in r disjoint parallel arcs, where $0 < r \leq p + q$, and D_2 the disk in ∂V_2 so that $rT(m,n)$ intersects D_2 in r disjoint parallel arcs, one for each component of $rT(m,n)$. Figure 1 shows the $(7,3)$-torus knot $T(7,3)$, 3 parallel copies $3T(1,1)$ of the $(1,1)$-torus knot, and the disks D_1 and D_2. We excise the disks D_1 and D_2 from their respective tori and glue the punctured tori together along their boundaries so that the orientations of $T(p,q)$ and $rT(m,n)$ align correctly. The resulting one must yield a knot in the boundary of a genus two handlebody H standardly embedded in S^3. Such a knot is called a *twisted torus knot*, which is denoted by $K(p,q,r,m,n)$. Figure 2 shows the twisted torus knot $K(7,3,3,1,1)$.

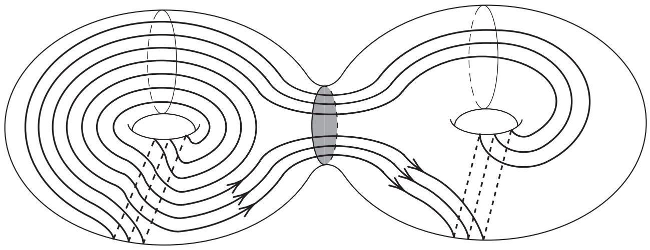

FIGURE 2. The twisted torus knot $K(7,3,3,1,1)$.

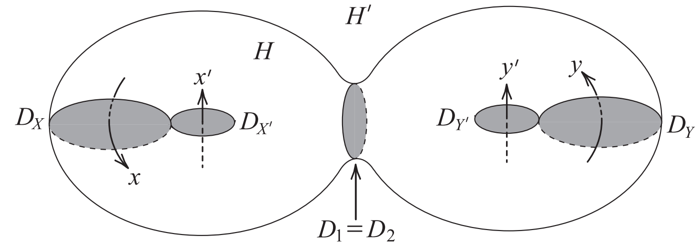

FIGURE 3. The generators of $\pi_1(H)$ and $\pi_1(H')$.

Let $H' = \overline{S^3 - H}$ and $\Sigma = \partial H = \partial H'$. Then $(H, H'; \Sigma)$ forms a genus two Heegaard splitting of S^3. Thus we can regard all of the twisted torus knots as lying on this genus two Heegaard surface Σ bounding the two handlebodies H and H' of S^3 as described above.

Proposition 2.2. *The surface slope of a twisted torus knot $K(p,q,r,m,n)$ with respect to the Heegaard surface Σ is $pq + r^2mn$.*

Proof. This is Proposition 3.1 in [6]. □

Let K be a twisted torus knot $K(p,q,r,m,n)$ lying in a genus two Heegaard splitting $(H, H'; \Sigma)$ of S^3. Let $w_{p,q,r,m,n}$ and $w'_{p,q,r,m,n}$ be the conjugacy class of K in $\pi_1(H) = \langle x, y\rangle$ and $\pi_1(H') = \langle x', y'\rangle$ respectively, where x and y are generators in H and x' and y' are generators in H', which are dual to the cutting disks as described in Figure 3. It easy to see that $w'_{p,q,r,m,n}$ is equal to $w_{q,p,r,n,m}$ with x replaced by x' and y replaced by y'. In addition by the construction of a twisted torus knot, $w_{p,q,r,m,n}$ ($w'_{p,q,r,m,n}$, resp.) does not depend on the parameter n (m, resp.). Therefore we often omit n (m, resp.).

There are more properties in $w_{p,q,r,m,n}$. For g and h in a group G, we say g is *equivalent* to h, denoted by $g \equiv h$, if there is an automorphism of G carrying g to h.

Lemma 2.3. *The words $w_{p,q,r,m}$ has the following properties.*

(1) $w_{p,q,r,m} \equiv w_{p,q',r,m}$ *if* $q \equiv \pm q' \mod p$.
(2) $w_{p,q,r,m} \equiv w_{p,q,r',m}$ *if* $r \equiv \pm r' \mod p$.

Proof. This is Lemma 3.3 in [6]. □

The following lemma and proposition show which values of the parameters p, q, r, m, and n produce a primitive or a Seifert curve of $K(p, q, r, m, n)$ with respect to H.

Lemma 2.4. *$w_{p,q,r,m}$ is primitive in $\pi_1(H)$ if and only if*

(1) $p = 1$; *or*
(2) $m = 1$ *and* $r = \pm 1$ *or* $\pm q \mod p$.

Proof. This is Theorem 3.4 in [6]. □

For integers p and q, we define $\hat{q}^{-1}$ be the smallest positive integer congruent to $\pm q^{-1} \mod p$. For a real number x, $\tilde{x}$ denotes the least integer function. In [6], Dean gave three criteria to determine which $w_{p,q,r,m}$ are Seifert-fibered in $\pi_1(H)$.

Proposition 2.5. *Let $w = w_{p,q,r,m}$ be a conjugacy class in $\pi_1(H)$ of a twisted torus knot $K(p, q, r, m, n)$, where $1 \le q < p/2$ and $1 \le r \le p$.*

(1) *If $m > 1$, $r \equiv \pm 1$ or $\pm q \mod p$, then w is (p, m) Seifert-fibered.*
(2) *If $m = 1$, $r \equiv \pm \beta q \mod p$, where $1 < \beta \le p/q$ with $p - \beta q > 1$, then w is $(\beta, p - \beta q)$ Seifert-fibered.*
(3) *If $m = 1$, $r \equiv \pm \bar{r} \mod p$, where $1 \le \bar{r} \le \widetilde{p/\hat{q}^{-1}}$, with $p - r\hat{q}^{-1} > 1$, then w is $(r, p - r\hat{q}^{-1})$ Seifert-fibered.*

For the twisted torus knot $K(p, q, r, m, n)$ with $p/2 < q < p$ or $p < r \le p+q$, we can apply Lemma 2.3. Thus we assume that $1 \le q < p$ and $1 \le r \le p + q$ in Proposition 2.5. According to [6], the first type (1), the second type (2), and the third type (3) of Seifert-fibered $w_{p,q,r,m}$ (or $K(p, q, r, m, n)$) in Proposition 2.5 are called *hyper Seifert-fibered, middle Seifert-fibered*, and *end Seifert-fibered* in H, respectively. Note that we can apply the lemma and proposition, and statements mentioned above by switching p and q, and m and n to say that $w'_{p,q,r,n}$ (or $K(p, q, r, m, n)$) is *hyper Seifert-fibered, middle Seifert-fibered*, or *end Seifert-fibered* in H'.

In this paper, we consider a twisted torus knot $K = K(p, q, r, m, n)$ which is hyper Seifert-fibered in H and middle Seifert-fibered in H'. In Section 3 we will find all possible values of the parameters p, q, r, m, and n for which K is hyper Seifert-fibered in H and middle Seifert-fibered in H'. If we let $H[K] = D^2(a, b)$ and $H'[K] = D^2(c, d)$, then by Lemma 1.1, Dehn surgery $K(\gamma)$ at the surface slope γ is either $S^2(a,b,c,d)$ or a graph manifold consisting of $D^2(a,b)$ and $D^2(c,d)$. However in Section 5 we will show that $K(\gamma)$ is a graph manifold by showing that two regular fibers of $H[K]$ and $H'[K]$ intersect in a single point in Σ.

3. Finding the parameters p, q, r, m, and n

In this section we find all possible values of the parameters p, q, r, m, and n for which $K(p,q,r,m,n)$ is hyper Seifert-fibered in H and middle Seifert-fibered in H'.

Theorem 3.1. *Let K be a twisted torus knot $K(p,q,r,m,n)$ lying in a genus two Heegaard splitting $(H,H';\Sigma)$ of S^3 with $1 \le q < p$, $\gcd(p,q)=1$, $m>1$, and $0<r\le p+q$. K is hyper Seifert-fibered in H and middle Seifert-fibered in H' if and only if the parameters p,q,r,m, and n satisfy one of the following values in Table 1. Table 2 describes $H[K]$ and $H'[K]$ explicitly.*

Table 1. All possible values of parameters p,q,r,m, and n for which $K(p,q,r,m,n)$ is hyper Seifert-fibered in H and middle Seifert-fibered in H'.

	(p,q,r,m,n)	satisfying
I	$(q+\bar{p}, q, q+2\bar{p}, m, \pm1)$	$0<\bar{p}<q$, $\lvert q-2\bar{p}\rvert>1$
II	$(iq+\epsilon, q, iq+2\epsilon, m, \pm1)$	$q>3, i>0, \epsilon=\pm1$ (if $\epsilon=-1$, then $i>1$)
III	$(iq+\bar{p}, (\beta+1)\bar{p}+\epsilon, p+\epsilon, m, \pm1)$	$\bar{p}>0, \beta>1, i>0, \epsilon=\pm1$ with $\bar{p}+\epsilon>1$
IV	$(iq-\bar{p}, (\beta+1)\bar{p}-\epsilon, p+\epsilon, m, \pm1)$	$\bar{p}>0, \beta>1, i>1, \epsilon=\pm1$ with $\bar{p}-\epsilon>1$

Table 2. $H[K]$ and $H'[K]$ when K is hyper Seifert-fibered in H and is middle Seifert-fibred in H'.

	(p,q,r,m,n)	$H[K]$	$H'[K]$
I	$(q+\bar{p}, q, q+2\bar{p}, m, \pm1)$	$D^2(p,m)$	$D^2(2, \lvert q-2\bar{p}\rvert)$
II	$(iq+\epsilon, q, iq+2\epsilon, m, \pm1)$	$D^2(p,m)$	$D^2(2, q-2)$
III	$(iq+\bar{p}, (\beta+1)\bar{p}+\epsilon, p+\epsilon, m, \pm1)$	$D^2(p,m)$	$D^2(\beta, \bar{p}+\epsilon)$
IV	$(iq-\bar{p}, (\beta+1)\bar{p}-\epsilon, p+\epsilon, m, \pm1)$	$D^2(p,m)$	$D^2(\beta, \bar{p}-\epsilon)$

Proof. We find all possible values of the parameters p,q,r,m, and n which satisfy the following two conditions simultaneously called the "hyper" condition and the "middle" condition which basically come from (1) and (2) in Proposition 2.5 respectively:

(1) the "hyper" condition: $m>1$, $r\equiv \pm1$ or $\pm q \mod p$; equivalently, $r=1$, q, $p-1$, $p+1$, $p-q$, $p+q$, or $2p-q$.
(2) the "middle" condition: $n=\pm1, r\equiv \pm\beta p' \mod q$, where $p\equiv \pm p' \mod q$ with $0<2p'<q$, $1<\beta<q/p'$, and $q-\beta p'>1$.

However there are restrictions on the parameters q and r which rule out some values of the parameters. If $q = 1$, or $r = eq \pm 1$, $eq - p$, or $p - eq$ for some integer e, then by Lemma 2.4 $w'_{p,q,r,n}$ is primitive on H'. Therefore all possible r satisfying the hyper condition (1) are as follows;

$$(1^*) \qquad r = p-1,\ p+1,\ q \text{ with } q > 1, \text{ or } 2p - q.$$

Regarding the condition (2), we need to find p' such that $p \equiv \pm p' \mod q$ with $0 < 2p' < q$. Thus if $p = iq + \bar{p}$, where $i > 0$ and $0 < \bar{p} < q$, then finding such a p' depends on the size of q and $\bar{p}$. If $q > 2\bar{p}$, then $p' = \bar{p}$ and $w'_{p,q,r,n} = w'_{\bar{p},q,r,n}$ is $(\beta, q - \beta\bar{p})$ Seifert-fibered. If $q < 2\bar{p}$, then we let $\bar{\bar{p}} = q - \bar{p}$. Thus $p = (i+1)q - \bar{\bar{p}}$ and $p \equiv -\bar{\bar{p}} \mod q$ with $0 < 2\bar{\bar{p}} < q$. Therefore in this case, $p' = \bar{\bar{p}}$ and $w'_{p,q,r,n} = w'_{\bar{\bar{p}},q,r,n}$ is $(\beta, q - \beta\bar{\bar{p}})$ Seifert-fibered. Note that $q \neq 2\bar{p}$, otherwise since $\gcd(p,q) = 1$, $\bar{p} = 1$ and $q = 2$, which is a contradiction to $q > 2p' \geq 2$.

As discussed above, we divide the argument into the two cases: $q > 2\bar{p}$ and $q < 2\bar{p}$.

Case 1: Suppose $q > 2\bar{p}$.

In the "middle" condition (2), $p' = \bar{p}$ and thus $r \equiv \pm\beta\bar{p} \mod q$, equivalently $r = jq \pm \beta\bar{p}$ with $1 < \beta < q/\bar{p}$, where j is an integer, and $w'_{p,q,r,n} \equiv w'_{\bar{p},q,r,n}$ is $(\beta, q - \beta\bar{p})$ Seifert-fibered. We divide this case into two subcases: $r = jq + \beta\bar{p}$ and $r = jq - \beta\bar{p}$, and find all possible values of the parameters by investigating which r also satisfies the values in the condition (1^*), i.e., $p + \epsilon, q$, or $2p - q$, where $\epsilon = \pm 1$.

Subcase 1: Assume $r = jq - \beta\bar{p}$. If $r = p + \epsilon$, then $jq - \beta\bar{p} = p + \epsilon$. Since $p = iq + \bar{p}$,

$$jq - \beta\bar{p} = iq + \bar{p} + \epsilon \Leftrightarrow (j - i)q = (\beta + 1)\bar{p} + \epsilon.$$

Since the right-hand side is positive, $j > i$. On the other hand, since $w'_{\bar{p},q,r,n}$ is $(\beta, q - \beta\bar{p})$ Seifert-fibered, the index condition implies that $q - \beta\bar{p} > 1$. From the equation $jq - \beta\bar{p} = iq + \bar{p} + \epsilon$, $q - \beta\bar{p} = (i - j + 1)q + \bar{p} + \epsilon$, which implies that $i - j + 1 \geq 0$ and thus $j \leq i + 1$. Therefore $j = i + 1$, $q = (\beta+1)\bar{p} + \epsilon$ and also $p = iq + \bar{p}$, $r = p + \epsilon$. This solution belongs to the type (III) in Table 1. Furthermore, $w_{p,q,r,m}$ is (p, m) Seifert-fibered and $w'_{p,q,r,n}$ is $(\beta, \bar{p} + \epsilon)$ Seifert-fibered.

If $r = q$, then $jq - \beta\bar{p} = q$ and equivalently $(j-1)q = \beta\bar{p}$. Since the right-hand side $\beta\bar{p}$ is positive, $j > 1$ and thus $q \leq \beta\bar{p}$, which is a contradiction to $1 < \beta < q/\bar{p}$.

If $r = 2p - q$, then $p < 2q$ because $0 < r < p + q$. In addition $i = 1$ in the equation $p = iq + \bar{p}$, i.e., $p = q + \bar{p}$. Therefore

$$jq - \beta\bar{p} = 2p - q \Leftrightarrow (j-1)q = (\beta+2)\bar{p}.$$

Since q and $\bar{p}$ are coprime, q must divide $\beta+2$. However the inequality $q - \beta\bar{p} > 1$ implies that $q = \beta+2$, $\bar{p} = 1$, and thus $j = 2$. Therefore $p = \beta+3$, $q = \beta+2$, and $r = \beta + 4$. This solution belongs to the solution (III) by putting $\bar{p} = 1$, $\epsilon = 1$, and $i = 1$ there.

Subcase 2: Assume $r = jq + \beta\bar{p}$. If $r = p + \epsilon$, then $jq + \beta\bar{p} = p + \epsilon$. Since $p = iq + \bar{p}$,

$$jq + \beta\bar{p} = iq + \bar{p} + \epsilon \Leftrightarrow (j - i)q = (1 - \beta)\bar{p} + \epsilon.$$

Since $(1-\beta)\bar{p}+\epsilon \leq 0$, $j \leq i$. On the other hand, from the inequality $q-\beta\bar{p} > 1$ and from the equation $jq + \beta\bar{p} = iq + \bar{p} + \epsilon$, $q - \beta\bar{p} = (j - i + 1)q - \bar{p} - \epsilon > 1$, which implies that $j - i + 1 > 0$ and thus $j > i - 1$. Therefore $j = i$ and thus from the equation $(j - i)q = (1 - \beta)\bar{p} + \epsilon$, $(1 - \beta)\bar{p} + \epsilon = 0$. This implies that $\beta = 2, \bar{p} = 1$, and $\epsilon = 1$. Therefore $p = iq + 1$ and $r = iq + 2$, which belongs to the type (II) in Table 1. Furthermore $w_{p,q,r,m}$ is (p, m) Seifert-fibered and $w'_{p,q,r,n}$ is $(2, q - 2)$ Seifert-fibered.

If $r = q$, then $jq + \beta\bar{p} = q$ and equivalently $(1 - j)q = \beta\bar{p}$. Since the right-hand side $\beta\bar{p}$ is positive, $j < 1$ and thus $q \leq \beta\bar{p}$, which is a contradiction to $1 < \beta < q/\bar{p}$.

If $r = 2p - q$, then as handled in the first subcase, $p < 2q$ and $p = q + \bar{p}$. Therefore

$$jq + \beta\bar{p} = 2p - q \Leftrightarrow (j - 1)q = (2 - \beta)\bar{p}.$$

Since the right-hand side $(2 - \beta)\bar{p}$ is nonpositive, $j \leq 1$. However if $j \leq 0$, then $q \leq (\beta - 2)\bar{p} < \beta\bar{p}$, which is a contradiction. Therefore $j = 1$ and thus $\beta = 2$, which implies that $p = q + \bar{p}$ and $r = q + 2\bar{p}$. This belongs to the type (I) in Table 1. Also, $w_{p,q,r,m}$ is (p, m) Seifert-fibered and $w'_{p,q,r,n}$ is $(2, q - 2\bar{p})$ Seifert-fibered.

Case 2: Suppose $q < 2\bar{p}$.

As discussed before, $p = (i + 1)q - \bar{\bar{p}}$, where $\bar{\bar{p}} = q - \bar{p}$. Since $2\bar{\bar{p}} < q$, in the "middle" condition (2) $p' = \bar{\bar{p}}$ and thus $r \equiv \pm\beta\bar{\bar{p}} \mod q$, equivalently $r = jq \pm \beta\bar{\bar{p}}$ with $1 < \beta < q/\bar{\bar{p}}$, where j is an integer, and $w'_{p,q,r,n} \equiv w'_{\bar{\bar{p}},q,r,n}$ is $(\beta, q - \beta\bar{\bar{p}})$ Seifert-fibered.

Subcase 1: Assume $r = jq - \beta\bar{\bar{p}}$. If $r = p + \epsilon$, then $jq - \beta\bar{\bar{p}} = p + \epsilon$. Since $p = iq + \bar{p}$ and $\bar{\bar{p}} = q - \bar{p}$,

$$jq - \beta(q - \bar{p}) = iq + \bar{p} + \epsilon \Leftrightarrow (\beta + i - j)q = (\beta - 1)\bar{p} - \epsilon.$$

Since $q > \bar{p}$, $i - j \leq -1$, i.e., $j \geq i + 1$. On the other hand, from the inequality $q-\beta\bar{\bar{p}} > 1$ and from the equation $jq-\beta\bar{\bar{p}} = iq+\bar{p}+\epsilon$, $q-\beta\bar{\bar{p}} = (i-j+1)q+\bar{p}+\epsilon > 1$, which implies that $i - j + 1 \geq 0$ and thus $j \leq i + 1$. Therefore $j = i + 1$ and $(\beta - 1)q = (\beta - 1)\bar{p} - \epsilon$, equivalently $(\beta - 1)(q - \bar{p}) = -\epsilon$. This implies that $\beta = 2, q - \bar{p} = 1$, and $\epsilon = -1$. Also $p = (i + 1)q - 1$ and $r = (i + 1)q - 2$. With $(i + 1)$ replaced by i, this belongs to the type (II) in Table 1. Moreover $w_{p,q,r,m}$ is (p, m) Seifert-fibered and $w'_{p,q,r,n}$ is $(2, q - 2)$ Seifert-fibered.

If $r = q$, then $jq - \beta\bar{\bar{p}} = q$ and equivalently $(j - 1)q = \beta\bar{\bar{p}}$. Since the right-hand side $\beta\bar{\bar{p}}$ is positive, $j > 1$ and thus $q \leq \beta\bar{\bar{p}}$, which is a contradiction to $1 < \beta < q/\bar{\bar{p}}$.

If $r = 2p - q$, then as before $p < 2q$ and $p = q + \bar{p}$. Therefore

$$jq - \beta(q - \bar{p}) = 2p - q \Leftrightarrow (j - \beta - 1)q = (2 - \beta)\bar{p}.$$

Since q and $\bar{p}$ are coprime and $q > \beta$, $\beta = 2$ and $j = 3$. Therefore $p = q + \bar{p}$, $r = q + 2\bar{p}$. This belongs to the type (I) in Table 1. Also $w_{p,q,r,m}$ is (p, m) Seifert-fibered and $w'_{p,q,r,n}$ is $(2, 2\bar{p} - q)$ Seifert-fibered.

Subcase 2: Assume $r = jq + \beta\bar{\bar{p}}$. If $r = p + \epsilon$, then $jq + \beta\bar{\bar{p}} = p + \epsilon$. Since $p = iq + \bar{p}$ and $\bar{\bar{p}} = q - \bar{p}$,

$$jq + \beta(q - \bar{p}) = iq + \bar{p} + \epsilon \Leftrightarrow (j + \beta - i)q = (\beta + 1)\bar{p} + \epsilon.$$

Since $q > \bar{p}$, $j < i + 1$. On the other hand,

$$q - \beta\bar{\bar{p}} = (1 - \beta)q + \beta\bar{p} = (j - i + 1)q - \bar{p} - \epsilon > 1.$$

This implies that $j - i + 1 > 0$ and thus $j > i - 1$. Therefore $j = i$ and thus from the equation $(j + \beta - i)q = (\beta + 1)\bar{p} + \epsilon$,

$$\beta q = (\beta + 1)\bar{p} + \epsilon \Leftrightarrow \beta(\bar{p} + \bar{\bar{p}}) = (\beta + 1)\bar{p} + \epsilon.$$

This implies that $\bar{p} = \beta\bar{\bar{p}} - \epsilon$ and $q = (\beta + 1)\bar{\bar{p}} - \epsilon$, and thus $p = (i + 1)q - \bar{\bar{p}}$, $q = (\beta+1)\bar{\bar{p}}-\epsilon$, and $r = p+\epsilon$. With $i+1$ and $\bar{\bar{p}}$ replaced by i and $\bar{p}$ respectively, this belongs to the type (IV) in Table 1. Also $w_{p,q,r,m}$ is (p, m) Seifert-fibered and $w'_{p,q,r,n}$ is $(\beta, \bar{p} - \epsilon)$ Seifert-fibered.

If $r = q$, then $jq + \beta\bar{\bar{p}} = q$ and equivalently $(1 - j)q = \beta\bar{\bar{p}}$. Since the right-hand side $\beta\bar{\bar{p}}$ is positive, $j < 1$ and thus $q \leq \beta\bar{\bar{p}}$, which is a contradiction to $1 < \beta < q/\bar{\bar{p}}$.

If $r = 2p - q$, then as before $p < 2q$ and $p = q + \bar{p}$. Therefore

$$jq + \beta(q - \bar{p}) = 2p - q \Leftrightarrow (j + \beta - 1)q = (\beta + 2)\bar{p}.$$

Since q and $\bar{p}$ are coprime and $q - \beta\bar{\bar{p}} > 1$, $q = \beta + 2$ and $\bar{p} = j + \beta - 1$. Also by replacing q by $\beta + 2$ in the inequality $q - \beta\bar{\bar{p}} > 1$, we see that $(\bar{\bar{p}} - 1)\beta < 1$ and thus $\bar{\bar{p}} = 1$ and $\bar{p} = q - 1 = \beta + 1$. From the equation $\bar{p} = j + \beta - 1$, we obtain that $j = 2$. Thus the solution is that $p = 2\beta + 3$, $q = \beta + 2$, and $r = 3\beta + 4$. However this solution belongs to the type (I) by putting $q = \beta + 2$ and $\bar{p} = \beta + 1$ there. □

4. R-R diagrams of twisted torus knots

In this section, we give a brief explanation on how to make R-R diagram of simple closed curves lying in the boundary of a genus two handlebody and then we transform a twisted torus knot $K(p, q, r, m, n)$ lying in a genus two Heegaard splitting $(H, H'; \Sigma)$ of S^3 into R-R diagrams. R-R diagrams were originally introduced by Osborne and Stevens in [10]. For the definition and properties of R-R diagrams, see [2].

Suppose two simple closed curves k_1 and k_2 lie in the boundary of a genus two handlebody H with $\{D_X, D_Y\}$ a complete set of cutting disks as shown in Figure 4. By considering two parallel separating curves, i.e., belt curves as shown in Figure 4, we decompose the boundary of H into two handles (once-punctured tori) F_X, F_Y, and one annulus $\mathcal{A}$, so that the two handles F_X and F_Y contain ∂D_X and ∂D_Y respectively. Figure 5 shows this decomposition.

Note from Figure 5 that there are three nonparallel bands of connections (parallel arcs) in F_X, each of which consists of one connection, and there are two nonparallel bands of connections in F_Y, one of which contains one connection and the other contains two.

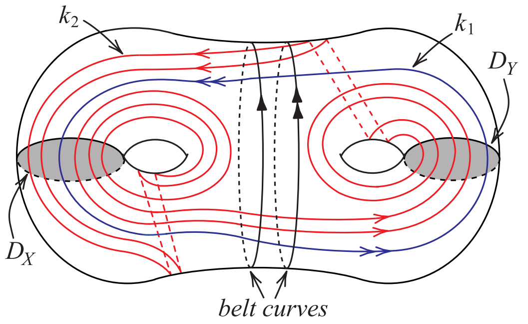

FIGURE 4. Belt curves bounding an annulus in a genus two surface.

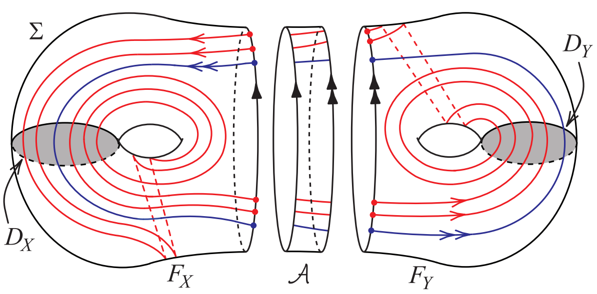

FIGURE 5. An annulus $\mathcal{A}$ and two handles F_X and F_Y.

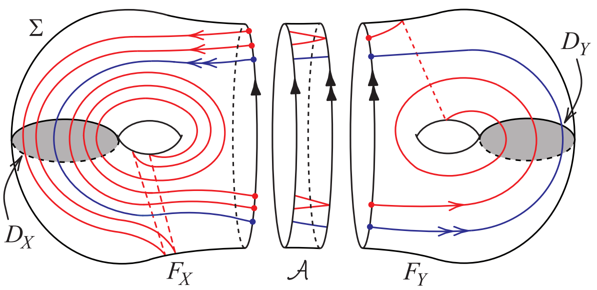

FIGURE 6. Merging the parallel connections and the endpoints of the arcs in the annulus $\mathcal{A}$.

Merging the parallel connections and thus the endpoints of the connections leads to mergers of the endpoints of arcs in the annulus $\mathcal{A}$ as in Figure 6. We observe from Figure 6 that after this merger, no pair of the arcs in $\mathcal{A}$ have the same endpoints and thus each arc has label 1.

With all of the information obtained, we can make an immersion of k_1 and k_2 into S^2 which becomes a corresponding R-R diagram. First embed the annulus $\mathcal{A}$ in S^2 in such a way that filling its boundary circles of $\mathcal{A}$ with disks, say $\mathcal{F}_X$ and $\mathcal{F}_Y$, yields S^2 as shown in Figure 7. $\partial\mathcal{F}_X$ and $\partial\mathcal{F}_Y$ correspond to ∂F_X and ∂F_Y respectively.

Now we immerse bands of connections in F_X and F_Y into $\mathcal{F}_X$ and $\mathcal{F}_Y$ as follows. Since there are three nonparallel bands of connections (parallel arcs) in F_X, and there are two nonparallel bands of connections in F_Y, these bands of connections correspond to three diameters in $\mathcal{F}_X$ and two in $\mathcal{F}_Y$ as shown in Figure 7. In order to put the labels of the endpoints of each diameter (or each band of connections), we consider ∂D_X and ∂D_Y in F_X and F_Y. Assume that all of the curves are oriented. Then the labels of the endpoints of each diameter on $\mathcal{F}_X$(or $\mathcal{F}_Y$) implies the intersection number with the cutting disk D_X (or D_Y). The labels of the endpoints of each diameter are given in Figure 7. We call a band of connections with one endpoint labeled by t and the other by $-t$ as t-connection or $(-t)$-connection. Sometimes we distinguish between t-connection and $(-t)$-connection to indicate which endpoint to emphasize.

Last, we disregard the boundary circles of $\mathcal{F}_X$ and $\mathcal{F}_Y$ and the negative labels of the endpoints of each connection in Figure 7 to obtain the corresponding R-R diagram. Figure 8 shows the curves k_1 and k_2 in ∂H and the corresponding R-R diagram. We put the capital letters **X** and **Y** in the R-R diagram to indicate correspondence to the two handles F_X and F_Y respectively and we call the corresponding handles as X-handle and Y-handle.

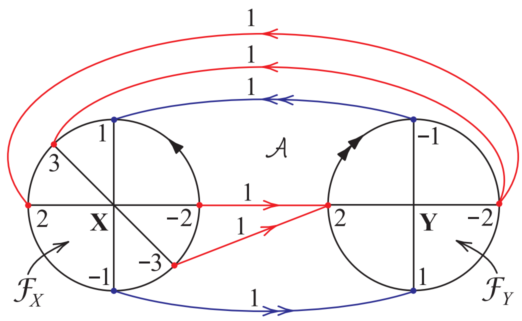

FIGURE 7. Immersion of the curves k_1 and k_2 into S^2 which becomes a corresponding R-R diagram.

R-R diagrams provide sufficient information about conjugacy classes of the element represented by a simple closed curve k in $\pi_1(H)$. $\pi_1(H)$ is a free group

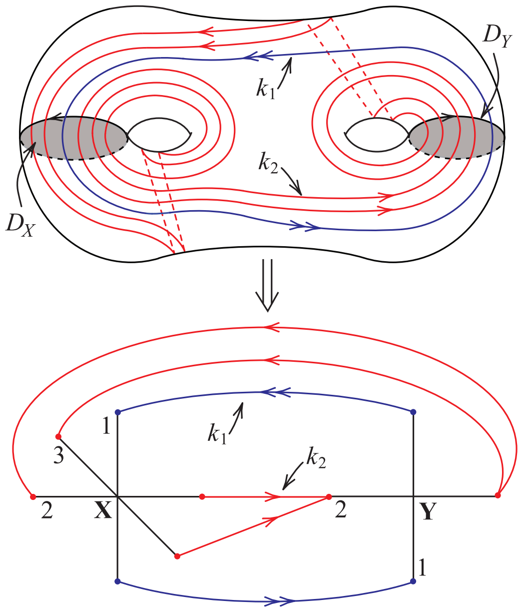

FIGURE 8. Transformation into R-R diagram.

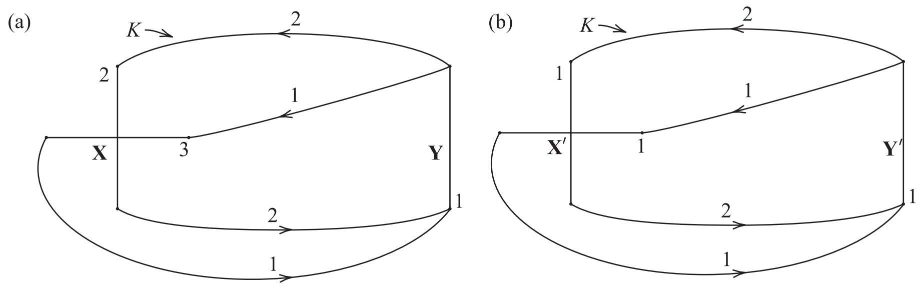

FIGURE 9. R-R diagrams of $K(7,3,3,1,1)$ with respect to H and H'.

$F(x, y)$ which is generated by x and y dual to the cutting disks D_X and D_Y respectively. In Figure 8, k_1 and k_2 represent the conjugacy classes of xy and $x^3y^2x^2y^2$ respectively in $\pi_1(H)$.

We are ready to make R-R diagram of a twisted torus knot $K = K(p, q, r, m, n)$. As an example, we use the twisted torus knot $K(7, 3, 3, 1, 1)$ in Figure 2 lying in the genus two Heegaard splitting $(H, H'; \Sigma)$ shown in Figure 3.

First we make R-R diagram of K with respect to the handlebody H. Take the boundary of the separating disk $D_1(= D_2)$ as one of the belt curves decomposing the boundary of H into two handles F_X and F_Y and use the complete set $\{D_X, D_Y\}$ of cutting disks of H dual to the generators x and y respectively in $\pi_1(H)$ for labelling the endpoints of each diameter in the R-R diagram. From the construction of K, $K \cap F_Y$ consists of r parallel arcs and thus there is only one band of connections in Y-handle. Also this band intersects the cutting disk D_Y m times, the label of the endpoint of the corresponding diameter is m. Also in Figure 2, $K(7, 3, 3, 1, 1) \cap F_X$ consists of two nonparallel bands of connections, one of which has two parallel arcs intersecting the cutting disk D_X twice and the other arc intersecting D_X three times. By putting all of the information above together, we have the R-R diagram of $K(7, 3, 3, 1, 1)$ with respect to H as shown in Figure 9a.

Similarly we make R-R diagram of K with respect to the handlebody H'. Take the boundary of the separating disk D_1 as one of the belt curves decomposing the boundary of H' into two handles $F_{X'}$ and $F_{Y'}$ and use the complete set $\{D_{X'}, D_{Y'}\}$ of cutting disks of H' dual to the generators x' and y' respectively in $\pi_1(H')$ for labelling the endpoints of each diameter in the R-R diagram. Note that since connections in each handle only depends on how they lie in the boundary of a genus two handlebody, R-R diagram of K with respect to H' has exactly the same form as that with respect to H, i.e., the same number of bands of connections in each handle and the same label of each edge. Only difference is the intersection numbers with the cutting disks in H and H'. Thus by considering the intersection numbers with the cutting disks $D_{X'}$ and $D_{Y'}$, we have the R-R diagram of K as shown in Figure 9b.

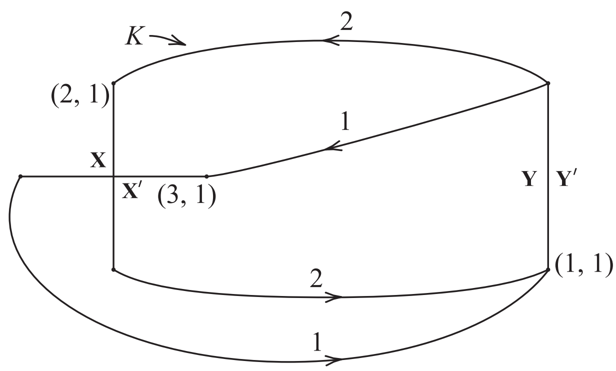

FIGURE 10. R-R diagram of $K(7, 3, 3, 1, 1)$ with respect to H and H'.

Since the two R-R diagrams have the same form, we put these into one R-R diagram as shown in Figure 10, where a pair of labels of the band of connections means that the first (second, resp.) coordinate is the label of R-R diagram with respect to H (H', resp.). In general, putting the two R-R diagrams into one R-R diagram is always doable because parallelism of arcs and connections rely only on the common boundary Σ of H and H'. Applying the argument in the

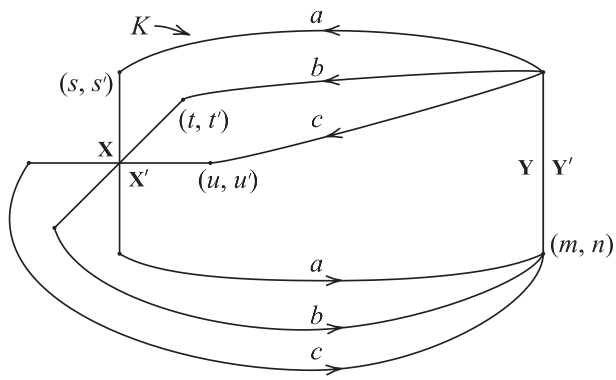

FIGURE 11. R-R diagram of $K(p,q,r,m,n)$ with respect to H and H', where $as+bt+cu = p$, $as'+bt'+cu' = q$, and $a+b+c=r$.

example of $K(7,3,3,1,1)$, we can obtain R-R diagram for a twisted torus knot $K(p,q,r,m,n)$ as shown in Figure 11, where $p = as+bt+cu$, $q = as'+bt'+cu'$, and $r = a+b+c$.

5. Twisted torus knots admitting graph manifold Dehn surgeries

In Section 3, using a twisted torus knot $K = K(p,q,r,m,n)$ we give four infinite families of Seifert/Seifert knots. These knots admit at a surface slope either $S^2(a,b,c,d)$ Dehn surgeries or graph manifold Dehn surgeries consisting of $D^2(a,b)$ and $D^2(c,d)$. In this section, we show that the four infinite families of Seifert/Seifert knots in Section 3 admit the latter. In order to show this, we need to figure out that regular fibers of $H[K] = D^2(a,b)$ and $H'[K] = D^2(c,d)$ intersect in the common boundary Σ of H and H'. To find regular fibers, we use R-R diagrams of K.

First, for $H[K]$ K lies in the boundary of H as a hyper Seifert-fibered curve. The following lemma shows how to find a regular fiber of $H[K]$.

Lemma 5.1. *Let $K = K(p,q,r,m,n)$ be a hyper Seifert-fibered curve in the boundary of a genus two handlebody H. Then the curve τ described in Figure* 12 *is a regular fiber of $H[K] = D^2(p,m)$.*

Proof. Recall that the genus two handlebody H is constructed from two standard solid tori V_1 and V_2 by gluing them along disks D_1 and D_2. ∂D_1 decomposes ∂H into two once-punctured tori F_X and F_Y which come from ∂V_1 and ∂V_2 respectively. Then $K \cap F_Y$ consists of r parallel arcs. As shown in Figure 13 using a band σ in F_Y which contains the r parallel arcs, and the disk D_1, we can construct a properly embedded separating essential annulus A in H. In other words, the annulus A can be obtained by bandsumming the disk D_1 with the band σ.

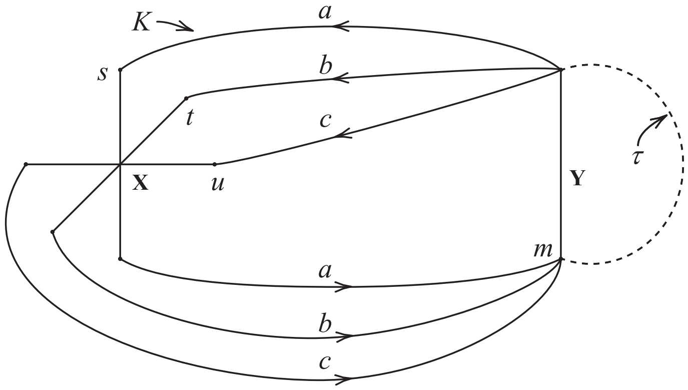

FIGURE 12. A regular fiber τ of $H[K] = D^2(p, m)$.

Cutting H apart along A yields a genus two handlebody W and a solid torus Z. Note that Z is homeomorphic to the solid torus V_2, and that K lies completely in the boundary of the genus two handlebody W as a twisted torus knot $K(p, q, r, 1, n')$ for some integer n'. Since $K(p, q, r, m, n)$ is hyper Seifert-fibered, $K(p, q, r, 1, n)$ is primitive in H. Also since the primitivity does not depend on the parameter n, by Lemma 2.4 $K(p, q, r, 1, n')$ is primitive in W, which implies that $W[K]$ is a solid torus. It follows that $H[K]$ is obtained by gluing the two solid tori $W[K]$ and Z together along A. So $H[K]$ is Seifert-fibered over D^2 with ∂A as regular fibers and the cores of $W[K]$ and Z as exceptional fibers. If we let τ be one boundary component of A, then τ is contained completely in F_Y and intersects the cutting disk D_Y m times. Thus τ appears as in the R-R diagram of K shown in Figure 12.

We further show that p and m are the indexes of the two exceptional fibers of $H[K]$. It is clear that the annulus A wraps around the solid torus Z m times longitudinally, so the core of Z is an exceptional fiber of index m. The other index can be obtained by computing $\pi_1(W[K][\tau])$. We can observe that $W[K][\tau]$ is homeomorphic to $W[\tau][K]$, $W[\tau]$ is a solid torus, and K lies in the boundary of $W[\tau]$ as a torus knot $T(p, q)$. Thus $\pi_1(W[K][\tau]) = \pi_1(W[\tau][K]) = \mathbb{Z}_p$ and then the core of $W[K]$ is an exceptional fiber of index p. □

The following lemma shows the geometric criterion for a simple closed curve k lying in the boundary of a genus two handlebody H to be Seifert and also geometric description of a regular fiber of $H[k]$.

Lemma 5.2. *If k is a nonseparating simple closed curve on the boundary of a genus two handlebody H such that $H[k]$ is Seifert-fibered over D^2 with two exceptional fibers, then k has an R-R diagram with the form of Figure* 14a, *with $n, s > 1$, or Figure* 14b *with $n > 0, s > 1$, $a, b > 0$, and* $\gcd(a, b) = 1$.

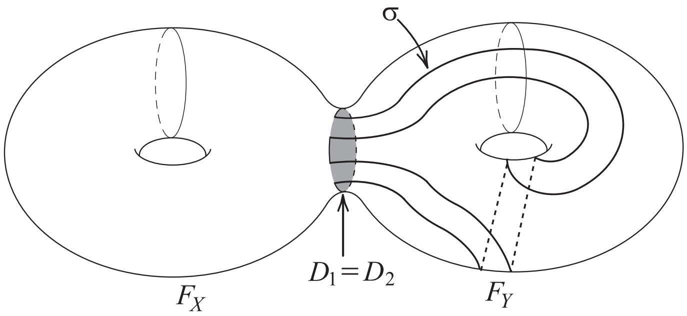

FIGURE 13. The separating essential annulus A in H which can be obtained by bandsumming the disk D_1 with the band σ.

Conversely, if k has an R-R diagram with the form of Figure 14a*, with $n, s > 1$, or Figure* 14b *with $n > 0, s > 1$, $a, b > 0$, and* $\gcd(a, b) = 1$*, then $H[k]$ is Seifert-fibered over D^2 with two exceptional fibers of indexes n and s, or indexes $n(a+b)+b$ and s respectively.*

In addition, the curves τ_1 and τ_2 in Figure 14a *and the curve τ in Figure* 14b *are regular fibers of $H[k]$.*

Proof. This is Theorem 3.2 in [4]. □

Remark. (1) Algebraically k in Figure 14a represents $x^n y^s$, while k in Figure 14b is the product of $x^n y^s$ and $x^{n+1} y^s$ with $|x^n y^s| = a$ and $|x^{n+1} y^s| = b$ in $\pi_1(H) = \langle x, y \rangle$. Here $|x^n y^s|$ denotes the total number of appearances of $x^n y^s$ in the word of k in $\pi_1(H)$, etc. Note that the exponents of x in k in Figure 14b differ by 1.

(2) The regular fibers τ_1 and τ_2 in Figure 14a of $H[k]$ represent x^n and y^s respectively, while the regular fiber τ in Figure 14b represents y^s in $\pi_1(H)$.

(3) If a curve disjoint from k in Figure 14a represents x^n (y^s, resp.), then this curve is isotopic to the curve τ_1 (τ_2, resp.) and thus can be a regular fiber of $H[k]$. Similarly if a curve disjoint from k in Figure 14b represents y^s, then this curve is isotopic to the curve τ_2 and thus can be a regular fiber of $H[k]$.

We use Lemma 5.2 and the remark above to find a regular fiber of $H'[K]$ for all of the types of a twisted torus knot $K = K(p, q, r, m, n)$ in Table 1.

Lemma 5.3. *Let $K = K(p, q, r, m, n)$ be a twisted torus knot lying in a genus two Heegaard splitting $(H, H'; \Sigma)$ of S^3 such that K is of type* I *in Table* 1*, i.e., $(p, q, r, m, n) = (q + \bar{p}, q, q + 2\bar{p}, m, \pm 1)$ with $0 < \bar{p} < q$ and $|q - 2\bar{p}| > 1$. Then at a surface slope γ, $K(\gamma)$ is a graph manifold consisting of $D^2(p, m)$ and $D^2(2, |q - 2\bar{p}|)$.*

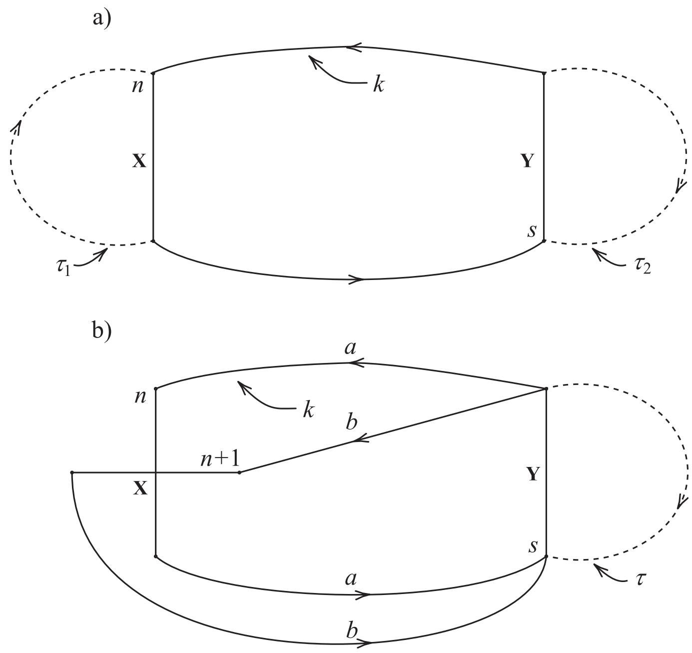

FIGURE 14. Two types of R-R diagrams of a Seifert-fibered curve k with $n, s > 1$ in Figure 14a, and $n > 0, s > 1$, $a, b > 1$, and $\gcd(a, b) = 1$ in Figure 14b, and regular fibers τ, τ_1, and τ_2 of $H[k]$.

Proof. By Theorem 3.1, K is hyper Seifert-fibered in H and middle Seifert-fibered in H' such that $H[K] = D^2(p, m)$ and $H'[K] = D^2(2, |q - 2\bar{p}|)$. Therefore it suffices to show that two regular fibers of $H[K]$ and $H'[K]$ intersect once. A regular fiber of $H[K]$ is understood in Lemma 5.1. In other words, it lies in Σ as shown in Figure 12. So we need to figure out how a regular fiber of $H'[K]$ lies in Σ.

We assume that $n = 1$. For the case where $n = -1$, the same argument can be applied. Let $q = \alpha\bar{p} + \bar{q}$, where $\alpha > 0$ and $0 \le \bar{q} < \bar{p}$ (if $\bar{q} = 0$, then $\bar{p} = 1$ because $\gcd(p, q)$=1). Then $p = (\alpha + 1)\bar{p} + \bar{q}$ and $r = (\alpha + 2)\bar{p} + \bar{q}$. Figure 15 shows the torus knot $T(p, q)$ lying in the boundary of a solid torus V_1 standardly embedded in S^3 and the disk D_1 containing r parallel arcs of $T(p, q)$ in V_1. It follows by figuring out nonparallel bands of connections in $F_1(= \overline{\partial V_1 - D_1})$ that K has an R-R diagram of the form shown in Figure 16a. Figure 16b shows R-R diagram of K when $\alpha = 3$.

Using the R-R diagram of K in Figure 16, we will find a regular fiber of $H'[K]$. We record the curve K algebraically by starting the $\bar{p}$ parallel arcs entering into the 1-connection in the X'-handle, i.e., entering into the endpoint

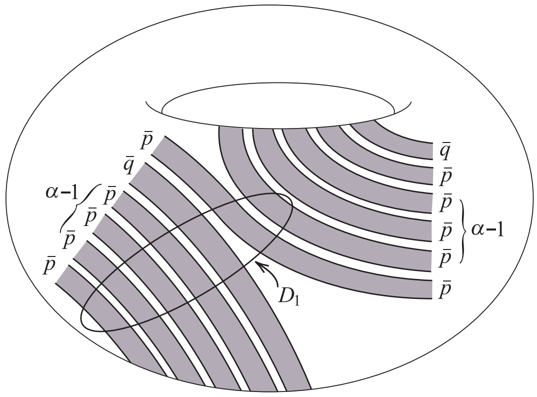

FIGURE 15. The torus knot $T(p, q)$ and the disk D_1 containing r parallel arcs of $T(p, q)$, where $p = (\alpha + 1)\bar{p} + \bar{q}$, $q = \alpha\bar{p} + \bar{q}$, and $r = (\alpha + 2)\bar{p} + \bar{q}$.

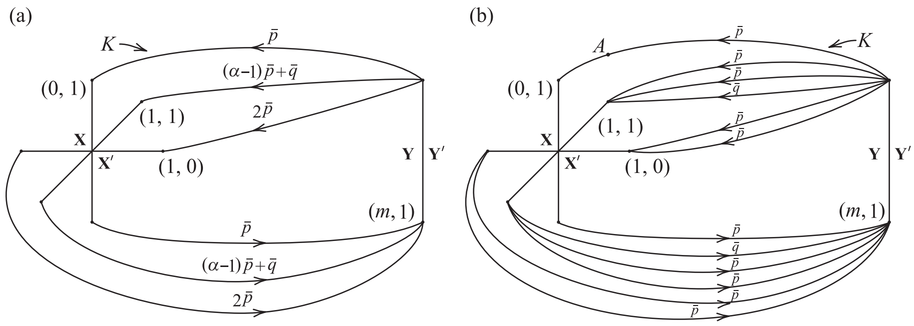

FIGURE 16. R-R diagram of K.

of the band of connections labeled by 1. In other words, in Figure 16b, we read off a word of K from the point A lying on $\bar{p}$ parallel edges entering into the 1-connection in the X'-handle.

Suppose $\alpha > 1$. Using the R-R diagram of K when $\alpha = 3$ in Figure 16b, we read off a word of K from the point A. The $\bar{p}$ parallel edges trace out $x'y'x'^0y'(x'y')^2\cdots$ and then after passing the Y'-handle four times they must split into two subsets of parallel edges, one of which has $\bar{q}$ parallel edges and the other has $\bar{p}-\bar{q}$ parallel edges. The $\bar{q}$ parallel edges trace out $x'y'x'^0y'$ while the $\bar{p}-\bar{q}$ parallel edges trace out x'^0y' before they come back to the starting point A. Therefore it follows that K is the product of two subwords

$$x'y'x'^0y'(x'y')^2x'y'x'^0y' = x'y'^2(x'y')^2x'y'^2 \text{ and}$$
$$x'y'x'^0y'(x'y')^2x'^0y' = x'y'^2(x'y')^1x'y'^2$$

with $|x'y'^2(x'y')^2x'y'^2| = \bar{q}$ and $|x'y'^2(x'y')^1x'y'^2| = \bar{p} - \bar{q}$. Similarly, for the R-R diagram of K in Figure 16a one can see that K is the product of two subwords

$$x'y'x'^0y'(x'y')^{\alpha-1}x'y'x'^0y' = x'y'^2(x'y')^{\alpha-1}x'y'^2 \text{ and}$$
$$x'y'x'^0y'(x'y')^{\alpha-1}x'^0y' = x'y'^2(x'y')^{\alpha-2}x'y'^2$$

with $|x'y'^2(x'y')^{\alpha-1}x'y'^2| = \bar{q}$ and $|x'y'^2(x'y')^{\alpha-2}x'y'^2| = \bar{p} - \bar{q}$.

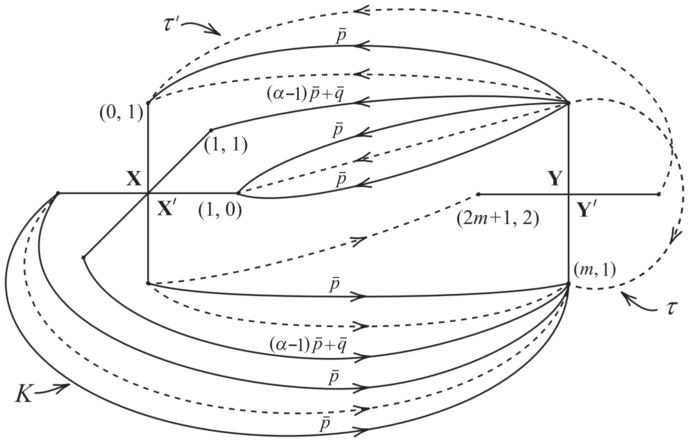

FIGURE 17. Regular fibers τ and τ' of $H[K]$ and $H'[K]$ respectively, which intersect each other in a single point.

We perform a change of cutting disks of the handlebody H' underlying the R-R diagram, which induces an automorphism of $\pi_1(H')$ that takes $x' \mapsto x'y'^{-1}$ and leaves y' fixed. Then by this change of cutting disks, $x'y'^2(x'y')^{\alpha-1}x'y'^2$ and $x'y'^2(x'y')^{\alpha-2}x'y'^2$ are sent to $x'y'x'^{\alpha}y'$ and $x'y'x'^{\alpha-1}y$ respectively. We perform another change of cutting disks of H' inducing an automorphism $y' \mapsto x'^{-1}y'$ to send $x'y'x'^{\alpha}y'$ and $x'y'x'^{\alpha-1}y$ to $y'x'^{\alpha-1}y'$ and $y'x'^{\alpha-2}y'$ respectively. So only 2 appears in the exponent of y' and the exponents of x' differ by 1. By Lemma 5.2 and the remark below Lemma 5.2, we see that a curve representing y'^2 is a regular fiber of $H'[K]$. Consider the curve τ' in the original R-R diagram of K as shown in Figure 17. τ' is disjoint from K. Also τ' represents $x'y'x'^0y'x'y'^2 (= x'y'^2x'y'^2)$ in $\pi_1(H')$, which is sent to y'^2 after performing the two automorphisms $x' \mapsto x'y'^{-1}$ and $y' \mapsto x'^{-1}y'$ consecutively as performed to K. Therefore by the remark (3) below Lemma 5.2, τ' is a regular fiber of $H'[K]$.

If $\alpha = 1$, we let $\bar{p} = \rho\bar{q} + \eta$, where $\rho > 0, 0 \leq \eta < \bar{q}$ (if $\eta = 0$, then $\bar{q} = 1$ and $\rho(= \bar{p}) > 2$ because $\gcd(p, q) = 1$ and $|q - 2\bar{p}| > 1$). By replacing $\bar{p}$ by $\rho\bar{q} + \eta$ in the R-R diagram and by recording the curve K algebraically by starting the $\bar{q}$ parallel arcs entering into the 1-connection in the X'-handle, we can observe that K is the product of two subwords

$$x'y'^2(x'y'^3)^{\rho-1}x'y'^3x'y'^2 \text{ and } x'y'^2(x'y'^3)^{\rho-1}x'y'^2$$

with $|x'y'^2(x'y'^3)^{\rho-1}x'y'^3x'y'^2| = \eta$ and $|x'y'^2(x'y'^3)^{\rho-1}x'y'^2| = \bar{q} - \eta$. We perform changes of cutting disks of the handlebody H' underlying the R-R diagram twice, which first induce an automorphism $x' \mapsto x'y'^{-3}$ and second induce an automorphism $y'^{-1} \mapsto x'^{-1}y'^{-1}$ of $\pi_1(H')$. Then $x'y'^2(x'y'^3)^{\rho-1}x'y'^3x'y'^2$ and $x'y'^2(x'y'^3)^{\rho-1}x'y'^2$ are sent to $y'^{-1}x'^{\rho}y^{-1}$ and $y'^{-1}x'^{\rho-1}y'^{-1}$ respectively. Therefore a curve representing y'^2 is a regular fiber of $H'[K]$. As discussed in the case where $\alpha > 1$, the curve τ' disjoint from K shown in Figure 17 represents $x'y'x'^0y'x'y'^2 (= x'y'^2x'y'^2)$ in $\pi_1(H')$, which is sent to y'^2 after performing the two automorphisms $x' \mapsto x'y'^{-3}$ and $y'^{-1} \mapsto x'^{-1}y'^{-1}$ consecutively. Therefore τ' is a regular fiber of $H'[K]$.

In both cases where $\alpha > 1$ and $\alpha = 1$, the curve τ' shown in Figure 17 is a regular fiber of $H'[K]$ and intersects a regular fiber τ of $H[K]$ in a single point as illustrated in Figure 17. This implies that $K(\gamma) \cong H[K] \cup_\partial H'[K]$ is a graph manifold consisting of $D^2(p, m)$ and $D^2(2, |q - 2\bar{p}|)$, where γ is a surface slope. This completes the proof. □

Notation. Let a_0 and b be oriented simple closed curves on a surface which intersect in a single point. We define $a = a_0b^m$ to be an oriented simple closed curve on the surface obtained by twisting a_0 about b m times.

Lemma 5.4. *Let $K = K(p, q, r, m, n)$ be a twisted torus knot lying in a genus two Heegaard splitting $(H, H'; \Sigma)$ of S^3 such that K is of type* II *in Table* 1*, i.e., $(p, q, r, m, n) = (iq + \epsilon, q, iq + 2\epsilon, m, \pm 1)$ where $q > 3, i > 0, \epsilon = \pm 1$ (if $\epsilon = -1$, then $i > 1$). Then at a surface slope γ, $K(\gamma)$ is a graph manifold consisting of $D^2(p, m)$ and $D^2(2, q - 2)$.*

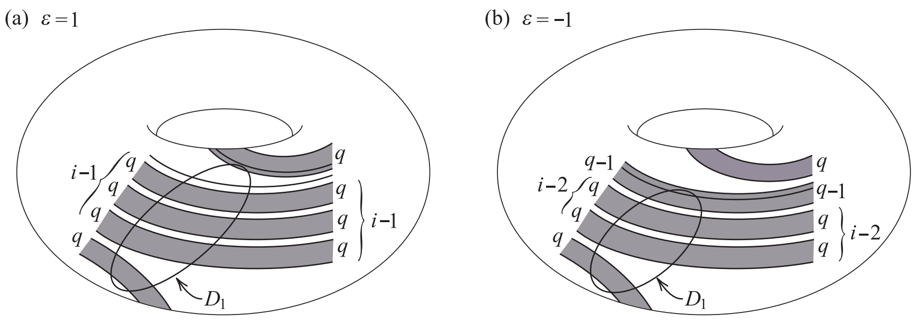

FIGURE 18. The torus knot $T(p, q)$ and the disk D_1 containing r parallel arcs of $T(p, q)$, where $p = iq + \epsilon$ and $r = iq + 2\epsilon$. Figures 18a and 18b show when $\epsilon = 1$ and $\epsilon = -1$ respectively.

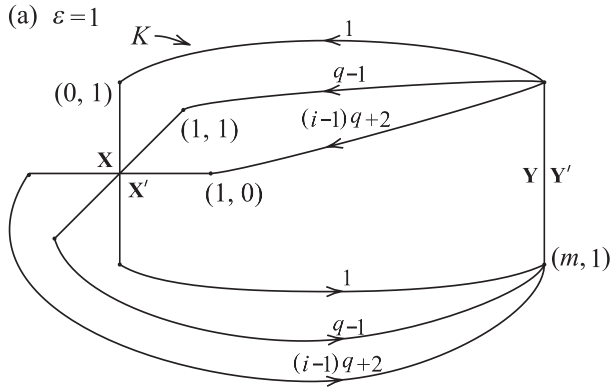

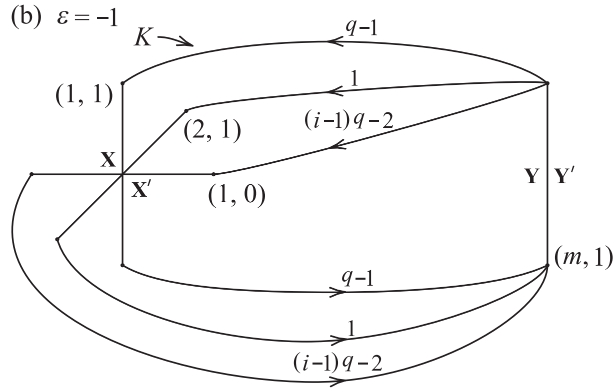

FIGURE 19. R-R diagram of K.

Proof. As in Lemma 5.3 we assume that $n = 1$. We need to figure out how a regular fiber of $H'[K]$ lies in Σ. Figure 18 shows the torus knot $T(p,q)$ and the disk D_1 containing r parallel arcs of $T(p,q)$ in V_1. It follows by figuring out nonparallel bands of connections in $F_1(=\overline{\partial V_1 - D_1})$ that K has an R-R diagram of the form shown in Figure 19.

First assume that $\epsilon = 1$. In the R-R diagram in Figure 19a by recording the curve K algebraically by starting the $q-1$ parallel arcs entering into the 1-connection in the X'-handle, we see that K is the product of two subwords

$$x'y'(x'^0y')^{i-1} = x'y'^i \text{ and}$$
$$x'y'(x'^0y')^{i-1}x'^0y'x'y'(x'^0y')^{i-1}x'^0y' = x'y'^{i+1}x'y'^{i+1}$$

with $|x'y'^i| = q-2$ and $|x'y'^{i+1}x'y'^{i+1}| = 1$. Therefore $K = (x'y'^i)^{q-2}(x'y'^{i+1})^2$. This can be shown by using an alternative R-R diagram of K shown in Figure 20a, where $K = K_1\lambda^{q-1}$, $K_1 = K_0\lambda_2^{i-1}$ and $\lambda = \lambda_1\lambda_2^{i-1}$. Note that from Figure 20a, since the curves K_0 and λ_1 intersect in a single point, $K_1 = K_0\lambda_2^{i-1}$

and $\lambda = \lambda_1 \lambda_2^{i-1}$ intersect in a single point. Therefore $K = K_1 \lambda^{q-1}$ is a simple closed curve.

In this description of K in Figure 20a we get by starting from the point P on K_0 that

$$K = x'y'x'^0y'(x'^0y')^{i-1}(x'y'(x'^0y')^{i-1})^{q-1}x'^0y' = (x'y'^i)^{q-2}(x'y'^{i+1})^2.$$

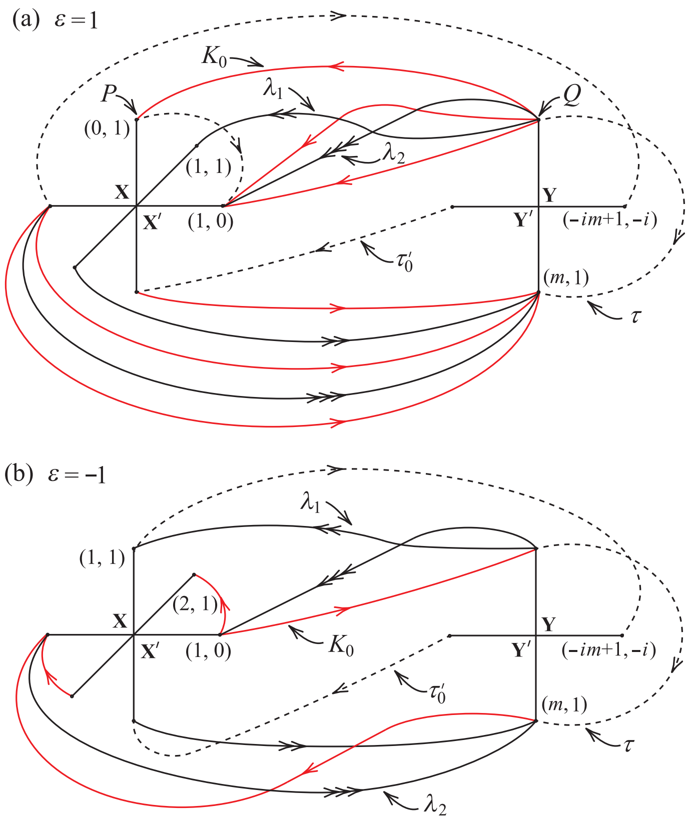

FIGURE 20. Alternative R-R diagram of K and regular fibers τ and τ' of $H[K]$ and $H'[K]$ respectively, which intersect each other in a single point. Here $\tau' = \tau_0' \lambda^{q-1}$ and $\lambda = \lambda_1 \lambda_2^{i-1}$.

To see that the alternative R-R diagram in Figure 20a is same as that of K in Figure 19a, it suffices to show that in both the R-R diagrams of K, the numbers of the parallel edges connecting the (X, X')-handle and the (Y, Y')-handle are equal. In Figure 20a, the number of parallel edges connecting the $(0, 1)$-connection in the (X, X')-handle and the $(-m, -1)$-connection in the (Y, Y')-handle (i.e., the points P and Q in Figure 20a) is 1 because only the curve K_0 connects the $(0, 1)$-connection and the $(-m, -1)$-connection once.

The number of parallel edges connecting the $(1,1)$-connection in the (X,X')-handle and the $(-m,-1)$-connection in the (Y,Y')-handle is equal to $q-1$ because these parallel edges result from the curve λ_1 and twisting about λ_1 is performed $q-1$ times to make K. The number of parallel edges connecting the $(1,0)$-connection in the (X,X')-handle and the $(-m,-1)$-connection in the (Y,Y')-handle is equal to $(i-1)q+2$ because these parallel edges result from the curves K_0 and λ_2, two of which are from K_0 and $(i-1)q$ parallel edges are from λ_2.

We perform two changes of cutting disks of the handlebody H' underlying the R-R diagram consecutively inducing automorphisms first $x' \mapsto x'y'^{-i}$ and second $y' \mapsto x'^{-q+1}y'$ of $\pi_1(H')$. Then $K = (x'y'^i)^{q-2}(x'y'^{i+1})^2$ is carried to $y'^2x'^{-q+2}$. This implies that a curve representing x'^{q-2} or y'^2 can be a regular fiber τ' in $H'[K]$. We take a curve representing x'^{q-2} as a regular fiber of $H'[K]$.

To find a regular fiber of $H'[K]$, we use the alternative R-R diagram of K in Figure 20a, where $K = K_1\lambda^{q-1}$, $K_1 = K_0\lambda_2^{i-1}$ and $\lambda = \lambda_1\lambda_2^{i-1}$. Consider a curve $\tau' = \tau_0'\lambda^{q-1}$, where τ_0' is given as in Figure 20a. Figure 20a shows that the curve τ_0' is disjoint from both K_0 and λ_2. This implies that τ_0' is disjoint from $K_1 = K_0\lambda_2^{i-1}$. In addition since K and τ' are obtained by twisting K_1 and τ_0' respectively about the same curve λ $q-1$ times, τ' is disjoint from K.

Algebraically τ' represents $x'^0y'^{-i}x'^{-1}(x'y'(x'^0y')^{i-1})^{q-1} = (x'y'^i)^{q-2}$ in $\pi_1(H')$, which is sent to x'^{q-2} after performing the two automorphisms $x' \mapsto x'y'^{-i}$ and $y' \mapsto x'^{-q+1}y'$ consecutively as performed to K. Therefore τ' is a regular fiber of $H'[K]$ and intersects a regular fiber τ of $H[K]$ in a single point as illustrated in Figure 20a.

Second assume that $\epsilon = -1$. Similarly by starting the $q-1$ parallel arcs entering into the 1-connection in the X'-handle from the R-R diagram in Figure 19b, we see that K is the product of two subwords

$$x'y'(x'^0y')^{i-2}x'^0y' = x'y'^i \text{ and}$$
$$x'y'(x'^0y')^{i-2}x'y'(x'^0y')^{i-2} = x'y'^{i-1}x'y'^{i-1}$$

with $|x'y'^i| = q-2$ and $|x'y'^{i-1}x'y'^{i-1}| = 1$. Therefore $K = (x'y'^i)^{q-2}(x'y'^{i-1})^2$. As in the case that $\epsilon = 1$, this can be checked by using an alternative R-R diagram of K shown in Figure 20b, where $K = K_1\lambda^{q-1}$, $K_1 = K_0\lambda_2^{i-1}$ and $\lambda = \lambda_1\lambda_2^{i-1}$. Then

$$K = x'^0x'x'^0y'^{-1}(y'(x'^0y')^{i-1}x')^{q-1}(y'x'^0)^{i-1} = (x'y'^i)^{q-2}(x'y'^{i-1})^2.$$

As in the case that $\epsilon = 1$, we can show that the alternative R-R diagram in Figure 20b is same as that of K in Figure 19b. In Figure 20b, the number of parallel edges connecting the $(1,1)$-connection in the (X,X')-handle and the $(-m,-1)$-connection in the (Y,Y')-handle is $q-1$ because these parallel edges result from the curve λ_1 and twisting about λ_1 is performed $q-1$ times to yield K. The number of parallel edges connecting the $(1,0)$-connection in the

(X, X')-handle and the $(-m, -1)$-connection in the (Y, Y')-handle is equal to $(i-1)q-2$. This is because $(i-1)q$ parallel edges result from the curve λ_2 but in the process of twisting K_0 about λ_2, one edge from $(i-1)q$ parallel edges is removed and also another edge becomes an edge connecting the $(2, 1)$-connection in the (X, X')-handle and the $(-m, -1)$-connection in the (Y, Y')-handle, which implies that there is one edge connecting the $(2, 1)$-connection and the $(-m, -1)$-connection.

Since $K = (x'y'^i)^{q-2}(x'y'^{i-1})^2$, we apply two automorphisms $x' \mapsto x'y'^{-i}$ and $y'^{-1} \mapsto x'^{-q+1}y'^{-1}$ of $\pi_1(H')$ consecutively. Then $K = (x'y'^i)^{q-2}(x'y'^{i-1})^2$ is carried to $y'^{-2}x'^{-q+2}$. This implies that a curve representing x'^{q-2} or y'^2 can be a regular fiber τ' in $H'[K]$. As in the case that $\epsilon = 1$, we take a curve representing x'^{q-2} as a regular fiber.

To find a regular fiber of $H'[K]$, we consider a curve $\tau' = \tau_0'\lambda^{q-1}$, where τ_0' is given as in Figure 20b. Since the two curves $K_1 = K_0\lambda_2^{i-1}$ and τ_0' are disjoint, and K and τ' are obtained by twisting K_1 and τ_0' respectively about the same curve λ $q-1$ times, τ' is disjoint from K. Also τ' represents $x'^{-1}y'^{-i}(y'(x'^0y')^{i-1}x')^{q-1} = (x'y'^i)^{q-2}$ in $\pi_1(H')$, which is sent to x'^{q-2} after performing the two automorphisms $x' \mapsto x'y'^{-i}$ and $y'^{-1} \mapsto x'^{-q+1}y'^{-1}$. Therefore τ' is a regular fiber of $H'[K]$ and intersects a regular fiber τ of $H[K]$ in a single point as illustrated in Figure 20b.

In both cases where $\epsilon = 1$ and $\epsilon = -1$, since τ and τ' intersect in a single point, $K(\gamma) \cong H[K] \cup_\partial H'[K]$ is a graph manifold consisting of $D^2(p, m)$ and $D^2(2, q-2)$. $\square$

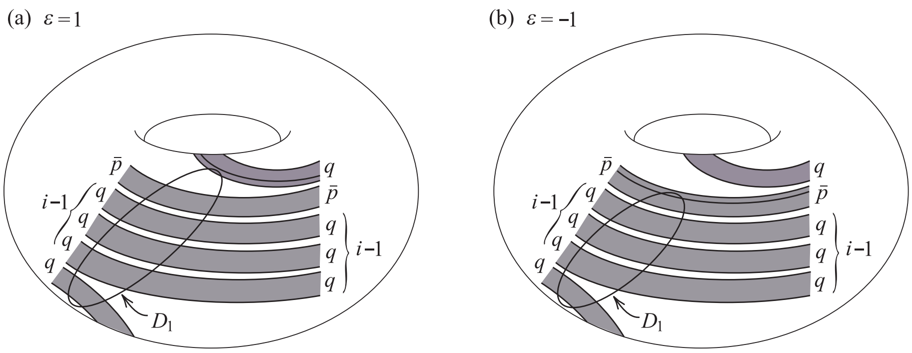

FIGURE 21. The torus knot $T(p, q)$ and the disk D_1 containing r parallel arcs of $T(p, q)$, where $p = iq + \bar{p}$, $q = (\beta+1)\bar{p} + \epsilon$, and $r = p + \epsilon$. Figures 21a and 21b show when $\epsilon = 1$ and $\epsilon = -1$ respectively.

Lemma 5.5. *Let $K = K(p, q, r, m, n)$ be a twisted torus knot lying in a genus two Heegaard splitting $(H, H'; \Sigma)$ of S^3 such that K is of type* III *in Table* 1*,* *i.e.*, $(p, q, r, m, n) = (iq+\bar{p}, (\beta+1)\bar{p}+\epsilon, p+\epsilon, m, \pm 1)$ *where* $\bar{p} > 0, \beta > 1, i > 0$, *and* $\epsilon = \pm 1$ *with* $\bar{p}+\epsilon > 1$. *Then at a surface slope* γ, $K(\gamma)$ *is a graph manifold consisting of* $D^2(p, m)$ *and* $D^2(\beta, \bar{p}+\epsilon)$.

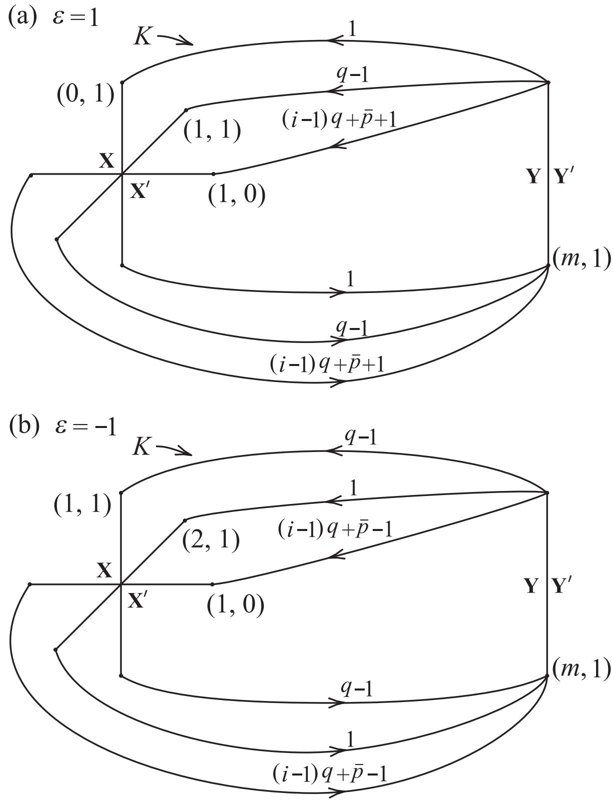

FIGURE 22. R-R diagram of K.

Proof. As before we assume that $n = 1$. Figure 21 shows the torus knot $T(p, q)$ and the disk D_1 containing r parallel arcs of $T(p, q)$ in V_1 and Figure 22 shows R-R diagram of K. Now we will find a regular fiber of $H'[K]$.

First assume that $\epsilon = 1$. In the R-R diagram in Figure 22a by recording the curve K algebraically by starting the $q-1(=(\beta+1)\bar{p})$ parallel arcs entering into the 1-connection in the X'-handle, we see that K is the product of three subwords

$$x'y'(x'^0y')^{i-1} = x'y'^i,\ x'y'(x'^0y')^{i-1}x'^0y' = x'y'^{i+1},\ \text{and}$$
$$x'y'(x'^0y')^{i-1}x'^0y'x'y'(x'^0y')^i = x'y'^{i+1}x'y'^{i+1}$$

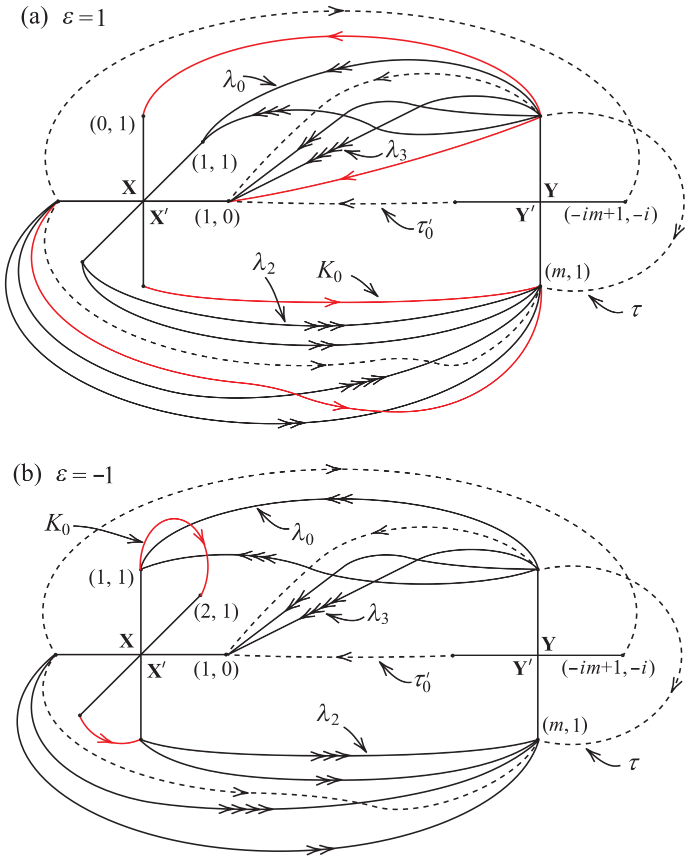

FIGURE 23. Alternative R-R diagram of K and regular fibers τ and τ' of $H[K]$ and $H'[K]$ respectively, which intersect each other in a single point. Here $\tau' = \tau_1'\lambda_1^{\beta}$, where $\tau_1' = \tau_0'\lambda_3^{i-1}$ and $\lambda_1 = \lambda_2\lambda_3^{i-1}$.

with $|x'y'^i| = \beta\bar{p}$, $|x'y'^{i+1}| = \bar{p}-1$, and $|x'y'^{i+1}x'y'^{i+1}| = 1$. Therefore $K = ((x'y'^i)^{\beta}(x'y'^{i+1}))^{\bar{p}}x'y'^{i+1}$. This is also guaranteed from an alternative R-R diagram of K shown in Figure 23a, where $K = K_1\lambda^{\bar{p}}$, where $K_1 = K_0\lambda_3^{i-1}$, $\lambda = \lambda_0^*\lambda_1^{\beta}$, $\lambda_0^* = \lambda_0\lambda_3^{i-1}$, and $\lambda_1 = \lambda_2\lambda_3^{i-1}$. Note from Figure 23a that since K_0 intersects λ_0 once and doesn't intersect λ_2, $K_1 = K_0\lambda_3^{i-1}$ intersects $\lambda_0^* = \lambda_0\lambda_3^{i-1}$ once and doesn't intersect $\lambda_1 = \lambda_2\lambda_3^{i-1}$. This implies that K_1 intersects $\lambda = \lambda_0^*\lambda_1^{\beta}$ in a single point, which shows that $K = K_1\lambda^{\bar{p}}$ is a simple closed curve.

The way of proving that the R-R diagram of K in Figure 23a is same as that of K in Figure 22a parallels that of proving that the two R-R diagrams of K in Figure 19a and in Figure 20a are identical in Lemma 5.4. Since we twist about λ_3 $((\beta+1)\bar{p}+1)(i-1)$ times and about λ_0 $\bar{p}$ times, and there is one edge induced from the curve K_0, there are a total of $((\beta+1)\bar{p}+1)(i-1)+\bar{p}+1 = (i-1)q+\bar{p}+1$ parallel edges connecting the $(1,0)$-connection in the (X,X')-handle and the $(-m,-1)$-connection in the (Y,Y')-handle. Similarly, there are a total of $(\beta+1)\bar{p} = q-1$ parallel edges connecting the $(1,1)$-connection in the (X,X')-handle and the $(-m,-1)$-connection in the (Y,Y')-handle, $\beta\bar{p}$ of which come from the curve λ_2 and the other $\bar{p}$ parallel edges come from the curve λ_0. There is only one edge connecting the $(0,1)$-connection in the (X,X')-handle and the $(-m,-1)$-connection in the (Y,Y')-handle, which results from the curve K_0.

From the alternative description of K in Figure 23a, we see that

$$\begin{aligned} K &= x'y'x'^0(y'x'^0)^{i-1}(y'x'y'(x'^0y')^{i-1}(x'y'(x'^0y')^{i-1})^{\beta}x'^0)^{\bar{p}}y' \\ &= ((x'y'^i)^{\beta}(x'y'^{i+1}))^{\bar{p}}x'y'^{i+1}. \end{aligned}$$

By performing two automorphisms $x' \mapsto x'y'^{-i}$ and $y' \mapsto x'^{-\beta-1}y'$ of $\pi_1(H')$ consecutively, we see that $K = ((x'y'^i)^{\beta}(x'y'^{i+1}))^{\bar{p}}x'y'^{i+1}$ is carried to $y'^{\bar{p}+1}x'^{-\beta}$. This implies that a curve representing x'^{β} or $y'^{\bar{p}+1}$ can be a regular fiber of $H'[K]$. We take a curve representing x'^{β} as a regular fiber.

To find a regular fiber of $H'[K]$, we use the alternative R-R diagram of K in Figure 23a, where a curve τ_0' is given. Using the curve τ_0', we can make a regular fiber of $H'[K]$. Consider a curve $\tau' = \tau_1'\lambda_1^{\beta}$, where $\tau_1' = \tau_0'\lambda_3^{i-1}$ and $\lambda_1 = \lambda_2\lambda_3^{i-1}$. We show that the curves K and τ' are disjoint. To see this, it suffices to show that τ' is disjoint from both K_1 and λ because $K = K_1\lambda^{\bar{p}}$, where $K_1 = K_0\lambda_3^{i-1}$, $\lambda = \lambda_0^*\lambda_1^{\beta}$, $\lambda_0^* = \lambda_0\lambda_3^{i-1}$, and $\lambda_1 = \lambda_2\lambda_3^{i-1}$. We see from Figure 23a that the curves τ_0' and λ_2 do not intersect K_0. Therefore $\tau_1' = \tau_0'\lambda_3^{i-1}$ and $\lambda_1 = \lambda_2\lambda_3^{i-1}$ do not intersect $K_1 = K_0\lambda_3^{i-1}$, which implies that $\tau' = \tau_1'\lambda_1^{\beta}$ is disjoint from K_1. Figure 23a shows that τ_0' doesn't intersect λ_0. Therefore $\tau_1' = \tau_0'\lambda_3^{i-1}$ doesn't intersect $\lambda_0^* = \lambda_0\lambda_3^{i-1}$. This implies that $\tau' = \tau_1'\lambda_1^{\beta}$ is disjoint from $\lambda = \lambda_0^*\lambda_1^{\beta}$.

Algebraically, τ' represents $x'^0(y'x'^0)^{i-1}y'(x'y'(x'^0y')^{i-1})^{\beta}x'^0y'^{-i} = (x'y'^i)^{\beta}$. This is sent to x'^{β} after the two automorphisms $x' \mapsto x'y'^{-i}$ and $y' \mapsto x'^{-\beta-1}y'$ of $\pi_1(H')$ as performed to K. Since τ' is disjoint from K and represents x'^{β}, τ' is a regular fiber of $H'[K]$. Figure 23a guarantees that the two regular fibers τ and τ' of $H[K]$ and $H'[K]$ intersect in a single point.

Second assume that $\epsilon = -1$. Similarly by starting the $q-1$ parallel arcs entering into the 1-connection in the X'-handle from the R-R diagram in Figure 22b, we see that K is the product of three subwords

$$\begin{aligned} &x'y'(x'^0y')^{i-1} = x'y'^i, \ x'y'(x'^0y')^{i-1}x'^0y' = x'y'^{i+1}, \text{ and} \\ &x'y'(x'^0y')^{i-1}x'y'(x'^0y')^{i-1} = x'y'^ix'y'^i \end{aligned}$$

with $|x'y'^i| = \beta\bar{p}-2$, $|x'y'^{i+1}| = \bar{p}-1$, and $|x'y'^ix'y'^i| = 1$. Therefore $K = (x'y'^{i+1}(x'y'^i)^{\beta})^{\bar{p}-1}(x'y'^i)^{\beta}$, which can also be verified as proved in the case that

$\epsilon = 1$ by using an alternative R-R diagram of K shown in Figure 23b, where $K = K_1\lambda^{\bar{p}-1}$, where $K_1 = K_0\lambda_1^{\beta}$, $\lambda = \lambda_0^*\lambda_1^{\beta}$, $\lambda_0^* = \lambda_0\lambda_3^{i-1}$, and $\lambda_1 = \lambda_2\lambda_3^{i-1}$. Also to show that the alternative R-R diagram of K is same as that of K in Figure 22b, we can apply the similar arguments as in the proof in Lemma 5.4 which shows that the two R-R diagrams of K in Figure 19b and in Figure 20b are identical.

By performing two automorphisms $x' \mapsto x'y'^{-i}$ and $y' \mapsto y'x'^{-\beta-1}$ of $\pi_1(H')$ consecutively, it follows that $(x'y'^{i+1}(x'y'^{i})^{\beta})^{\bar{p}-1}(x'y'^{i})^{\beta}$ is carried to $x'^{\beta}y'^{\bar{p}-1}$. This implies that a curve representing x'^{β} or $y'^{\bar{p}-1}$ can be a regular fiber τ' in $H'[K]$. We take a curve representing x'^{β} as a regular fiber.

Using the curve τ_0' depicted in Figure 23b, we make a curve $\tau' = \tau_1'\lambda_1^{\beta}$, where $\tau_1' = \tau_0'\lambda_3^{i-1}$ and $\lambda_1 = \lambda_2\lambda_3^{i-1}$. We observe from Figure 23b that the curve τ_0' doesn't intersect K_0 and λ_0, and λ_3 doesn't intersect K_0. Therefore $\tau_1' = \tau_0'\lambda_3^{i-1}$ is disjoint from K_0 and $\lambda_0^* = \lambda_0\lambda_3^{i-1}$. This implies that $\tau' = \tau_1'\lambda_1^{\beta}$ is disjoint from $K_1 = K_0\lambda_1^{\beta}$ and $\lambda = \lambda_0^*\lambda_1^{\beta}$. Thus the curve τ' is disjoint from the curve K.

Algebraically, τ' represents $x'^0(y'x'^0)^{i-1}y'(x'y'(x'^0y')^{i-1})^{\beta}x'^0y'^{-i} = (x'y'^{i})^{\beta}$. This is sent to x'^{β} after the two automorphisms $x' \mapsto x'y'^{-i}$ and $y' \mapsto y'x'^{-\beta-1}$ of $\pi_1(H')$ as performed to K. Since τ' is disjoint from K and represents x'^{β}, τ' is a regular fiber of $H'[K]$. From Figure 23b the two regular fibers τ and τ' of $H[K]$ and $H'[K]$ respectively intersect in a single point.

In both cases where $\epsilon = 1$ and $\epsilon = -1$, since the regular fibers τ and τ' respectively intersect in a single point, $K(\gamma) \cong H[K] \cup_\partial H'[K]$ is a graph manifold consisting of $D^2(p, m)$ and $D^2(\beta, \bar{p} + \epsilon)$. □

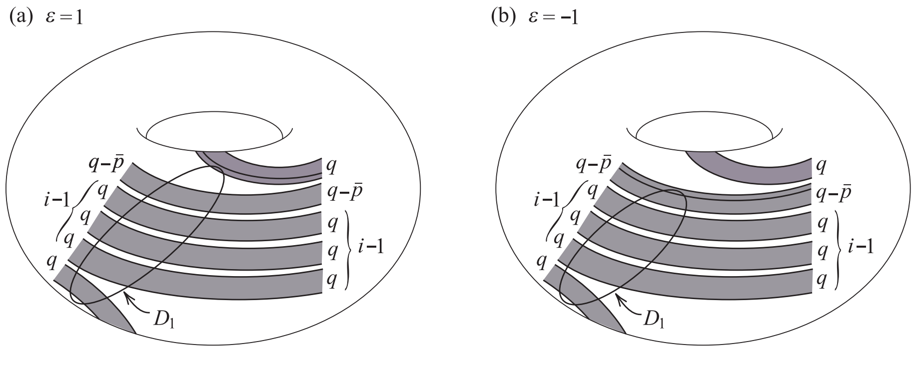

FIGURE 24. The torus knot $T(p, q)$ and the disk D_1 containing r parallel arcs of $T(p, q)$, where $p = iq - \bar{p}$, $q = (\beta + 1)\bar{p} - \epsilon$, and $r = p + \epsilon$. Figures 24a and 24b show when $\epsilon = 1$ and $\epsilon = -1$ respectively.

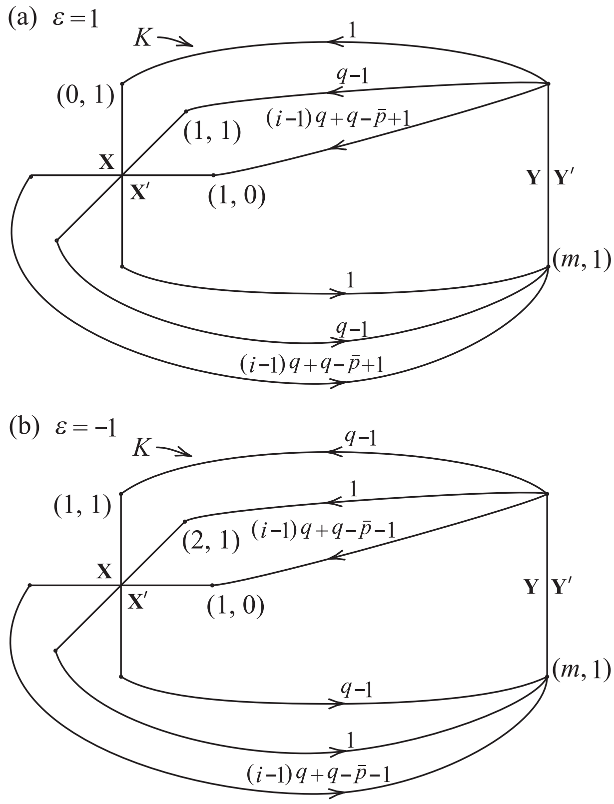

FIGURE 25. R-R diagram of K.

Lemma 5.6. *Let $K = K(p, q, r, m, n)$ be a twisted torus knot lying in a genus two Heegaard splitting $(H, H'; \Sigma)$ of S^3 such that K is of type* IV *in Table* 1*, i.e., $(p, q, r, m, n) = (iq - \bar{p}, (\beta+1)\bar{p} - \epsilon, p + \epsilon, m, \pm 1)$ where $\bar{p} > 0, \beta > 1, i > 1$, and $\epsilon = \pm 1$ with $\bar{p} - \epsilon > 1$. Then at a surface slope γ, $K(\gamma)$ is a graph manifold consisting of $D^2(p, m)$ and $D^2(\beta, \bar{p} - \epsilon)$.*

Proof. Figure 24 shows the torus knot $T(p, q)$ and the disk D_1 containing r parallel arcs of $T(p, q)$ in V_1 and Figure 25 shows R-R diagram of K. The R-R diagram of K in Figure 25 is same as that of K in Figure 22 which is of type III, with $q - \bar{p}$ replace by $\bar{p}$. So the proof is similar as that in Lemma 5.5. □

By Lemmas 5.3, 5.4, 5.5, and 5.6 we obtain the main theorem of this paper as follows.

Theorem 5.7. *There are infinite families of Seifert/Seifert knots in S^3 admitting a graph manifold consisting of $D^2(a, b)$ and $D^2(c, d)$. Furthermore, for any natural numbers $a, b, c,$ and d with $a \geq 3$ and $b, c, d \geq 2$, there are*

Seifert/Seifert knots in S^3 admitting a graph manifold consisting of $D^2(a,b)$ and $D^2(c,d)$.

Acknowledgements. The author would like to thank the referee for pointing out errors in the original texts and valuable comments and suggestions.

References

[1] J. Berge, *Some Knots with Surgeries Yielding Lens Spaces*, Unpublished manuscript. Univ. of Texas at Austin, 1990.

[2] ———, *A classification of pairs of disjoint nonparallel primitives in the boundary of a genus two handlebody*, arXiv:0910.3038.

[3] J. Berge and S. Kang, *The hyperbolic* $\mathrm{P/P}$, $\mathrm{P/SF_d}$, *and* $\mathrm{P/SF_m}$ *knots in* S^3, preprint.

[4] ———, *Primitive and Seifert curves in a genus two handlebody*, preprint.

[5] J. Dean, *Hyperbolic knots with small Seifert-fibered Dehn surgeries*, Ph.D. thesis, University of Texas at Austin, 1996.

[6] ———, *Small Seifert-fibered Dehn surgery on hyperbolic knots*, Algebr. Geom. Topol. **3** (2003), 435–472.

[7] M. Eudave-Muñoz, *Band sums of links which yield composite links. The cabling conjecture for strongly invertible knots*, Trans. Amer. Math. Soc. **330** (1992), no. 2, 463–501.

[8] ———, *Non-hyperbolic manifolds obtained by Dehn surgery on hyperbolic knots*, Proceedings of the 1993 International Georgia Topology Conference, W. Kazea (Ed.), 35–61, AMS/IP Stud. Adv. Math., 2.1, Amer. Math. Soc., Providence, RI, 1997.

[9] S. Kang, *Knots admitting Seifert-fibered surgeries over S^2 with four exceptional fibers*, to appear in Bull. Korean Math. Soc.

[10] R. P. Osborne and R. S. Stevens, *Group presentations corresponding to spines of 3-manifolds II*, Trans. Amer. Math. Soc. **234** (1977), no. 1, 213–243.

[11] D. Rolfsen, *Knots and Links*, Math. Lect. Ser. **7**, Publish or Perish, Berkeley, California, 1976.

[12] M. Teragaito, *Hyperbolic knots with three toroidal Dehn surgeries*, J. Knot Theory Ramifications **17** (2008), no. 9, 1051–1061.

Department of Mathematics Education
Chonnam National University
Gwangju 500-757, Korea
E-mail address: skang4450@chonnam.ac.kr